

SPECTROSCOPIC CONFIRMATION OF THE PISCES OVERDENSITY¹

JUNA A. KOLLMEIER², ANDREW GOULD³, STEPHEN SHECTMAN², IAN B. THOMPSON², GEORGE W. PRESTON², JOSHUA D. SIMON², JEFFREY D. CRANE², ŽELJKO IVEZIĆ⁴, & BRANIMIR SESAR⁴

Draft version November 1, 2018

ABSTRACT

We present spectroscopic confirmation of the “Pisces Overdensity”, also known as “Structure J”, a photometric overdensity of RR Lyrae stars discovered by the Sloan Digital Sky Survey (SDSS) at an estimated photometric distance of ~ 85 kpc. We measure radial velocities for 8 RR Lyrae stars within Pisces. We find that 5 of the 8 stars have heliocentric radial velocities within a narrow range of $-87 \text{ km s}^{-1} < v_r < -67 \text{ km s}^{-1}$, suggesting that the photometric overdensity is mainly due to a physically associated system, probably a dwarf galaxy or a disrupted galaxy. Two of the remaining 3 stars differ from one another by only 9 km/s, but it would be premature to identify them as a second system.

Subject headings: Galaxy: halo, Galaxy: structure, galaxies: dwarf, stars: RR Lyrae

1. INTRODUCTION

In the currently favored picture of galactic structure formation, the Milky Way had a tumultuous early history. Continuously bombarded from an early age by other galaxies big and small, the Milky Way has been roiled by mergers — a picture first put forth by Searle & Zinn (1978). The fossil record of the Milky Way’s history can be seen today in the debris left over from this cosmic carnage — the stellar streams that appear to be the shredded remains of galaxies past. The SDSS has had a major impact in breaking open this field. A variety of photometric techniques have been developed to search through the large photometric database of the SDSS to uncover these systems (e.g. Newberg et al. 2002, Willman et al. 2005, Belokurov et al. 2006, Grillmair et al. 2006). The primary search algorithms rely on a combination of correlations in position on the sky and position in the color-magnitude diagram (CMD). To date, a significant number of such structures have been located. However, the census of structures is still very far from complete, particularly at large Galactocentric distances. The key issue is sensitivity: at very low intrinsic luminosities these objects can only be disentangled from foreground stars interior to ~ 50 kpc and SDSS star counts are only sensitive to surface brightnesses above $\sim 30 \text{ mag/arcsec}^{-2}$. A novel technique, first recognized by Kinman & Wirtanen (1963), to push the limits of finding substructure within the Milky Way is to make use of the photometric variability of RR Lyrae stars.

The repeated scans of SDSS Stripe-82 have allowed the discovery of Milky Way substructures via their populations of RR Lyrae stars, which are standard candles, can be seen to large distances, and show distinctive light curves. The structure discussed in this *Letter* was first

identified as an overdensity of RR Lyrae stars by Sesar et al. (2007) as part of a larger study of all RR Lyrae stars in Stripe-82. They termed this overdensity “Structure J”, one among several such structures located. In a subsequent work, Watkins et al. (2009) independently found what appears to be the same structure, which they termed the “Pisces Overdensity”. The photometric identification of these overdensities is a crucial first step in locating more streams and galaxies interior to the virial radius of the Milky Way. However, photometry provides two phase-space dimensions very accurately (angular position) and a third only very crudely (distance). In order to show definitively whether photometric overdensities are, in fact, truly part of a common structure as opposed to a chance concentration, it is necessary to obtain data for additional phase-space dimension(s), which could in principle be either radial velocities or proper motions (e.g., Simon et al. 2007). In this *Letter*, we report on the first results of a campaign to confirm distant structures in the Milky Way halo as defined by RR Lyrae and giant stars.

2. OBSERVATIONS

2.1. Target Selection

In Figure 1 we show all of the identified RR Lyrae stars in the apparent magnitude range $19.9 \leq V_0 \leq 20.8$ that lie in SDSS Stripe-82, which covers a $3^\circ \times 118^\circ$ stripe along the celestial equator. The positions and V_0 magnitudes of these objects come from the latest Stripe-82 RR Lyrae catalog (Sesar et al. 2009). There is a very clear overdensity in the RA interval 335–360. With only about 30% of the stripe area, this sub-region contains 24 of the 31 RR Lyrae stars (77%). For our first campaign we focused on the concentration located at $RA \sim 355^\circ$ and selected 8 objects near this overdensity based on their close 2D proximity and their similar median magnitudes.

2.2. Light Curve Analysis

Obtaining a single-epoch spectrum for an RR Lyrae star yields only a velocity of the stellar photosphere, which for these pulsating variables can deviate from the systemic velocity by several 10s of km s^{-1} . However,

¹ This paper includes data gathered with the 6.5 meter Magellan Telescopes located at Las Campanas Observatory, Chile.

² Observatories of the Carnegie Institution of Washington, 813 Santa Barbara Street, Pasadena, CA 91101

³ Department of Astronomy, The Ohio State University, 4051 McPherson Laboratory, Columbus, OH, 43210

⁴ Department of Astronomy, University of Washington, Box 351580, Seattle, WA 98195-1580

the dense temporal sampling of Stripe-82 enables us to obtain accurate ephemerides by phase folding the ~ 70 epochs in the SDSS photometric archive. We can then correct velocity measurements made at known phase to the barycentric velocities for these stars (Joy 1938). We extracted the lightcurves from the SDSS archive and determined their periods based on a variant of the “Phase Dispersion Minimization” technique (Stellingwerf 1978). We first identified potential bad data points by performing a regression on g vs. r flux, and flagging 2.5σ outliers (as determined from the scatter – not the formal errors). While the colors of RR Lyrae stars change during their pulsation cycle, the 2.5σ criterion allows an adequate range for normal color variation. We then removed near-achromatic points that were substantially fainter than the remaining points, which are probably due to some joint photometric anomaly, but in any case would not fit any RR Lyrae-like light curve. Finally, we varied the period and minimized the sum of the squares of the photometric differences between successive points. Our derived g -band lightcurves for our 8 target objects are shown in Figure 2. In all but one case, periods derived from the g -band data were nearly identical to periods derived from the r -band data. Based on these differences, we estimate the period error to be $\sigma(P) = 3 \times 10^{-6}$ day. Interestingly, our derived periods are surprisingly similar, with a dispersion of only 0.026 days. The objects are all RRAb type variables and with median brightnesses of about $g \sim 20.5$ these stars are at a distance of about 85 kpc. We have also estimated metallicities using the periods and amplitudes for the 8 stars using equation (6) of Sandage (2004), assuming that the V -band amplitude is equal to the g -band amplitude. The metallicities range from $[Fe/H] \sim -1.3$ to -2.1 . While these estimates are necessarily crude, we can conclude that all of the 8 stars are relatively metal-poor.

2.3. Spectroscopic Observations

The spectroscopic observations were obtained using the Magellan Echelle Spectrograph (MagE⁵; Marshall et al. 2008) mounted on the 6.5-m Clay Telescope at Las Campanas Observatory. In all cases two equal-length exposures bracketed an observation of a ThAr lamp. The data were reduced using a pipeline written by D. Kelson following Kelson (2003). Post-extraction processing of the spectra was done with the IRAF⁶ ECHELLE package. A 1-arcsec slit was used, resulting in a resolution of ~ 4100 , and the signal-to-noise ratio of the final spectra ranged from 7 to 16 per 0.36\AA pixel at 4700\AA . Exposure times varied from 3600s to 4000s depending on the observing conditions. Velocities were measured with the IRAF FXCOR routine using a MagE observation of the blue metal-poor star CS22874-009 ($V_{helio} = -36.6 \text{ km s}^{-1}$, Preston & Sneden 2000) as the template. The cross correlations were made on the wavelength interval $4000\text{\AA} - 5600\text{\AA}$ with the hydrogen lines masked out.

We adopt the time-averaged velocity of the pulsation

⁵ <http://www.lco.cl/telescopes-information/magellan/instruments/mage7>

⁶ IRAF is distributed by the National Optical Astronomy Observatories, which are operated by the Association of Universities for Research in Astronomy, Inc., under a cooperative agreement with the NSF.

curve as the center-of-mass velocity of the star. Integration of detailed velocity curves of the RRA variables WY Ant, XZ Aps, DT Hya, and RV Oct (Preston 2009, in preparation) shows that the pulsation velocity is equal to the star’s time-average velocity at phase 0.37, reckoned relative to maximum light. Our observations were all made as close to this phase as possible, and velocity corrections were applied adopting $k = 92.7 \text{ km s}^{-1}$ per unit phase for the mean slope of the pulsation velocity curve at phase 0.37 for these four stars.

A journal of the observations is presented in Table 1. Column one lists the heliocentric Julian date at mid-observation followed by the RA and Dec of the star, the median g -band magnitude, the adopted pulsation period, the observed heliocentric velocity and the error as estimated from the FXCOR measurement, the number of photometric datapoints in the lightcurve, the heliocentric Julian date at maximum light (zero phase), the pulsation phase at mid-observation, the velocity correction, and the final adopted heliocentric velocity.

3. RESULTS

We were able to obtain accurate radial velocity measurements for 8 RR Lyrae stars associated within the apparent Pisces Overdensity. We show in Figure 3 a histogram of the heliocentric radial velocities measured for our targets. There is a clear velocity peak, containing 5 of the 8 objects, at approximately -75 km s^{-1} . The other 3 stars also have an interesting velocity distribution to which we return later. Figure 4 shows our targets coded by velocity and magnitude. We also show in this figure other RR Lyrae stars identified in the field (Sesar et al. 2009) fainter than $V_0 = 20$. The spatial concentration at $(RA, DEC) \sim (355^\circ, -0.3^\circ)$ is suggestive of a coherent structure. However, our radial velocity measurements reveal a more nuanced picture. One of these objects (cyan square) has an apparent magnitude that puts it farther out in the halo than the rest of the concentration. The three central stars (marked as triangles in the figure) within this concentration have measured radial velocities⁷ $-198 \text{ km s}^{-1} < v_r < -155 \text{ km s}^{-1}$. Four stars in the central concentration and a fifth further away, however, have radial velocities that lie within the main velocity peak. We therefore seem to have two co-spatial velocity structures, one robustly identified in phase-space and one that is suggestive but too sparsely sampled at present to warrant detailed analysis. While few data exist at these distances in the stellar halo, a Besançon model (Robin et al. 2003) of the heliocentric velocity distribution at this position in the sky suggests that the expected velocity distribution of the smooth stellar halo is centered at $\sim -120 \text{ km s}^{-1}$ with a dispersion of $\sim 90 \text{ km s}^{-1}$. In Section 4, we focus exclusively on the main velocity peak.

4. DISCUSSION

4.1. Is the Velocity Group Physically Associated?

In order to determine the random chance that a grouping of 5 out of 8 stars could have velocities within

⁷ The single object with differing g -band and r -band period has a barycentric velocity of -197.7 km s^{-1} if the g -band period is adopted and -182.7 km s^{-1} if the r -band period is adopted.

20 km s⁻¹ of one another, we performed a Monte Carlo test by random samplings from a Gaussian distribution with dispersion of 90 km s⁻¹. We find this probability to be less than 0.6%. This is a fair test (and not an a posteriori justification of a curious velocity structure found serendipitously) because this corresponds to exactly the velocity signature we were looking for when we undertook the observations. The group is therefore physically associated at high confidence in a fully Bayesian sense.

4.2. Bound or Unbound?

When looking at the spatial and kinematic information, the first question one must ask is whether these stars are part of a bound or unbound system, i.e., is this an intruding galaxy, or the extended debris of a galaxy/star cluster? While information on more stars (e.g. giants and horizontal branch stars), would be important to address this question fully, some simple estimates are useful in providing guidance.

If the system is assumed to be bound, we can estimate the mass using a virial estimator (e.g., Heisler et al. 1985; Gould 1993):

$$M_{VT} = \frac{3\pi}{2G} \frac{\sigma^2}{\langle 1/R_{\perp,ij} \rangle_{i \neq j}} \quad (1)$$

where σ is the velocity dispersion of the system, $R_{\perp,ij}$ is the projected distance between each two stars. In order to measure the velocity dispersion we must account for the errors in our velocities. There are two main (identifiable) sources of velocity error. The primary source of uncertainty is the error due to the signal-to-noise ratio, which is reported in Table 1. A secondary source of uncertainty comes from our imprecise knowledge of the zero phase point due to the finite sampling of the Stripe-82 data. This error is $k/(\sqrt{2N}) = 65 \text{ km s}^{-1}/N$ where N is the number of data points in each light curve. For our data, this has a maximum value of 1 km s⁻¹ and therefore does not affect our dispersions significantly. The phase errors induced by the period errors are similar.

Assuming all 5 stars in the main velocity structure are part of the same physical structure, we obtain a velocity dispersion of $6.8_{-2.6}^{+3.9} \text{ km s}^{-1}$ which yields a mass of $1.4_{-0.7}^{+1.7} \times 10^8 M_{\odot}$. A more conservative possibility is that only the “clump” of four stars near (RA,Dec) = (356°, -0.3°) is part of a bound structure, from which the star at $\sim 352^\circ$ either has been tidally stripped or is not physically associated with the main structure. In this case, Equation (1) yields $8.5_{-5.4}^{+14.3} \times 10^7 M_{\odot}$, whose 1σ range is not far from the typical value of $1 \times 10^7 M_{\odot}$ for the mass interior to 300 pc found by Strigari et al. (2008) for dwarfs with a wide range of luminosities. Moreover, the apparent 0.5° radius of the concentration corresponds to about 750 pc, rather than 300 pc, and this difference could account for the level of discrepancy in mass. Hence, this structure is possibly virialized, and if so represents a new satellite of the Milky Way. Given the small number of confirmed stars and the large physical size, however, we cannot at this point rule out the possibility that it is being (or has been) tidally disrupted.

If the apparent structure is physical (and not a chance superposition) then whether it is bound or not, the presence of 4 RR Lyrae stars within a $\sim 0.5 \text{ deg}^2$ rectan-

gle implies that there must be a concentration of other stars within the system. By the fuel consumption theorem, S_{RR} , the RR Lyrae specific frequency (the number per V -band luminosity, normalized to $M_{V,\text{norm}} = -7.5$; Suntzeff et al. 1991) can be cast in terms of the fraction of He burning that takes place within RR Lyrae stars, η_{RR} :

$$S_{RR} = \frac{m_{\text{He}} - m_{\text{C}}/3}{4m_{\text{H}} - m_{\text{He}}} \frac{\eta_{RR}}{1 - \eta_{\text{He}}} 10^{0.4\Delta M_{\text{bol}}} = 360\eta_{RR} \quad (2)$$

where m_X is the atomic mass of X , $\eta_{\text{He}} \sim 25\%$ is the initial abundance of He, $\Delta M_{\text{bol}} = M_{V,RR} - M_{V,\text{norm}} + \Delta\text{BC}$, $M_{V,RR} = 0.6$, and $\Delta\text{BC} = 0.45$ is the difference in bolometric corrections between RR Lyrae stars and typical giant stars. The highest observed value is $S_{RR} = 158$ (Siegel et al. 2001), i.e., $\eta_{RR} = 0.44$. The surface brightness of the Pisces concentration may be expressed as $V = (34.0 + 2.5 \log \eta_{RR}) \text{ mag arcsec}^{-2}$, and hence to be “recognizable” as a $V = 30 \text{ mag arcsec}^{-2}$ overdensity would require $\eta_{RR} < 0.025$ or $S_{RR} < 9$. Such systems do exist (Harris et al. 1996), but they are far from universal. We cannot therefore, probe whether the Pisces structure is a physical (or chance) association based on the presence (or absence) of an already known photometric counterpart in giants. Deeper imaging data of this region as well as further spectroscopic follow-up of giant and horizontal branch stars in this region of the sky is necessary to confront this hypothesis.

4.3. Unbound Case: Galaxy or Globular Cluster?

If the object is an unbound stream, as opposed to a bound system, we must ask whether this represents the disrupted remnant of a globular cluster system or the remnant of a satellite galaxy. Robust characterization of streams and disrupting galaxies, both theoretically and observationally, is a challenge. The predicted phase-space morphology depends on a variety of initial conditions including initial mass, M/L ratio, stellar density profile and orbit parameters, and the observations are demanding and not always conducive to multiplexing due to the low density of targets. A thin physical extent transverse to the direction of motion on the sky, uniform stellar color-magnitude diagram and narrow velocity dispersion would typically indicate a globular cluster stream as opposed to a galaxy stream. The large width of our structure suggests that if it is disrupting, it is a satellite galaxy as opposed to a globular cluster. The velocity dispersion is comparable to what is observed within the Sagittarius stream (Majewski et al. 2004) or within the Anticenter Stream (Grillmair, Carlin & Majewski 2008).

If the Pisces Overdensity is indeed a disrupted satellite it is interesting that located near the central core of this structure are three stars with similar velocities but offset from the main structure by nearly 100 km s⁻¹. As such large velocity offsets are not plausible simply by disruption effects alone, these stars are either a separate, perhaps bound, structure or they are random interlopers. The latter scenario is of little interest. In the former scenario it is intriguing, but perhaps not surprising, that we observe two overlapping streams at this position in the halo. More locally, the Sagittarius system is so extensive and has made a sufficiently large number of orbits that many objects have been found within it (e.g. Segue 1)

that can only be disentangled using velocity and metallicity information. Farther out in the Galaxy, Bell et al. (2008) have determined that at least 50% of the stellar density is in a clumpy form. Detailed comparison with cosmologically-motivated models for the spaghetti-like nature of the halo would be useful in determining whether such self-overlapping systems are rare or commonplace in the Milky Way at these distances.

5. CONCLUSIONS

We present spectroscopic confirmation of the photometric overdensity observed in RR Lyrae stars toward the constellation Pisces. We suggest that this system is a dwarf galaxy – possibly in the process of disruption, possibly already disrupted, or possibly bound with very low surface brightness.

The nature of the stellar halo at distances of ~ 100 kpc is still relatively uncharted territory. Using RR Lyrae

stars to explore this regime of phase space is a novel and exciting way forward. Large photometric datasets such as those provided by SDSS and similar experiments in conjunction with large ground-based telescopes to obtain spectra should yield important insight into the nature of the Milky Way’s perhaps troubled, perhaps tranquil past.

We thank the participants of the KITP program “Building the Milky Way” where this project was hatched. A.G. was supported by NSF grant AST-0757888. I.B.T. was supported by NSF grant AST-0507325. This research was supported in part by the National Science Foundation under Grant No. PHY05-51164. JAK thanks Andy McWilliam, John Mulchaey, James Buckwalter, and Luis Saenz for stimulating discussions.

REFERENCES

- Bell, E. F., et al. 2008, *ApJ*, 680, 295
 Belokurov, V., et al. 2006, *ApJ*, 642, L137
 Gould, A. 1993, *ApJ*, 403, 37
 Grillmair, C. J., & Dionatos, O. 2006, *ApJ*, 643, L17
 Grillmair, C. J., Carlin, J. L., & Majewski, S. R. 2008, *ApJ*, 689, L117
 Harris, W.E., 1996, *AJ*, 112, 1487
 Heisler, J., Tremaine S., & Bahcall, John N., 1985, *ApJ*, 298, 8
 Joy, A., 1938, *PASP*, 50, 302
 Kelson, D. D. 2003, *PASP*, 115, 688.
 Kinman & Wirtanen 1963, *ApJ*, 137, 698.
 Majewski, S. R., Kunkel, W.E., Law, D.R., Polak, A.A., Rocha-Pinto, H.J., Crane, J.D., Frinchaboy, P.M., Hummels, C.B., Johnston, K.V., Patterson, R.J., Rhee, J., Skrutskie, M.F. & Weinberg, M.D. 2004a, *AJ*, 128, 245
 Marshall, J. L., et al. 2008, *Proc. SPIE*, 7014,
 Newberg, H. J., et al. 2002, *ApJ*, 569, 245
 Preston, G.W. & Sneden, C., 2000, *AJ*, 210, 1014
 Robin, A. C., Reylé, C., Derrière, S., & Picaud, S. 2003, *A&A*, 409, 523
 Sandage, A. 2004, *AJ*, 128, 858
 Searle, L., & Zinn, R. 1978, *ApJ*, 225, 357
 Sesar B. et al., 2007, *AJ*, 134, 2236
 Sesar B., et al., 2009, *ApJ* submitted
 Siegel et al., 2001, *AJ*, 121, 935
 Simon, J. D., & Geha, M. 2007, *ApJ*, 670, 313
 Stellingwerf, R.F., 1978, *ApJ*, 224, 953
 Strigari, L. E., Bullock, J. S., Kaplinghat, M., Simon, J. D., Geha, M., Willman, B., & Walker, M. G. 2008, *Nature*, 454, 1096
 Suntzeff, N., Kinman, T.D, Kraft, Robert P., 1991, *ApJ*, 367, 528
 Watkins et al. 2009 *MNRAS*, in press, arXiv:0906.0498
 Willman, B., et al. 2005, *AJ*, 129, 2692

TABLE 1
RR LYRAE TARGETS

HJD	RA	DEC	g_{med}	P_g	$v_{r,obs}$	N_{phot}	HJD $_{\Theta,0}$	Θ_{obs}	Δv	$v_{r,bar}$
5043.8323	352.46991	-1.17125	20.545	0.5973118	-62.8 (4.8)	65	3352.5903	0.422	-4.8	-67.6
5042.9037	356.29469	-0.80489	20.655	0.5955986	-73.0 (3.8)	84	4008.7571	0.315	5.1	-67.9
5012.8432	355.75079	-0.17316	20.603	0.5938712	-65.1 (3.3)	74	3270.7662	0.425	-5.1	-70.2
5013.9018	355.57762	-0.00838	20.628	0.5949283	-81.9 (3.6)	80	2911.7877	0.388	-1.7	-83.6
5044.8612	355.60088	-0.62351	20.524	0.6314823	-83.5 (4.9)	142	3635.7693	0.404	-3.2	-86.7
5042.8593	354.11676	-0.38425	20.569	0.6016641	-156.2 (6.1)	70	4418.7158	0.362	0.7	-155.5
5014.8779	354.87899	-0.15772	20.569	0.5902998	-191.6 (4.3)	74	3668.7372	0.436	-6.1	-197.7
5012.8932	354.95545	-0.27631	20.607	0.5310617	-191.7 (4.2)	66	3996.7940	0.335	3.2	-188.5

NOTE. — Periods derived in g and r -bands were identical for all but 1 star. In that case the velocity changes from -197.7 km s^{-1} to -182.7 km s^{-1} . Quoted velocities are heliocentric and values in parenthesis are the estimated observational errors.

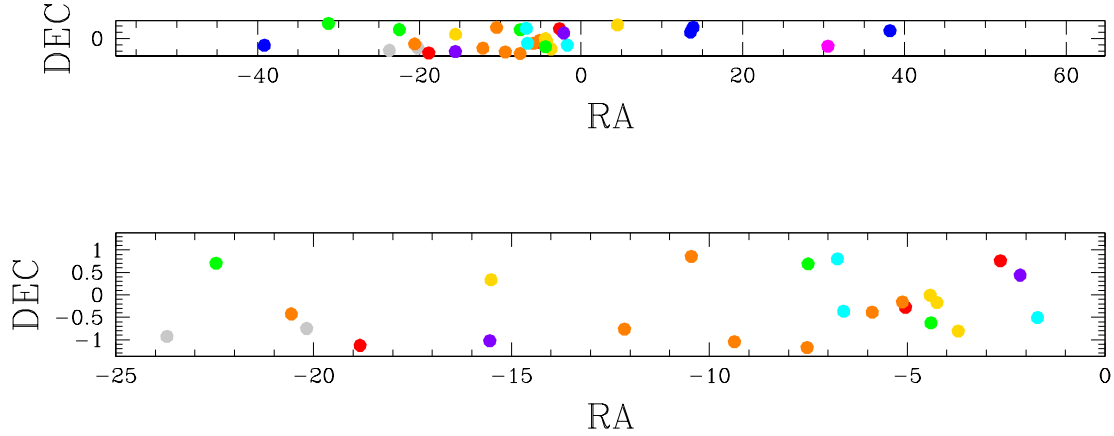


FIG. 1.— RR Lyrae stars in Stripe-82. **Top Panel:** positions of RR Lyrae stars with magnitudes $19.9 < V_0 < 20.8$ in the SDSS Stripe-82, color coded in 0.1 mag intervals, brightest to faintest: (gray, red, orange, yellow, green, cyan, blue, magenta, purple). Notice the extreme concentration at RA $-25^\circ - 0^\circ$. **Bottom Panel:** Zoom of Panel A in the region of the concentration.

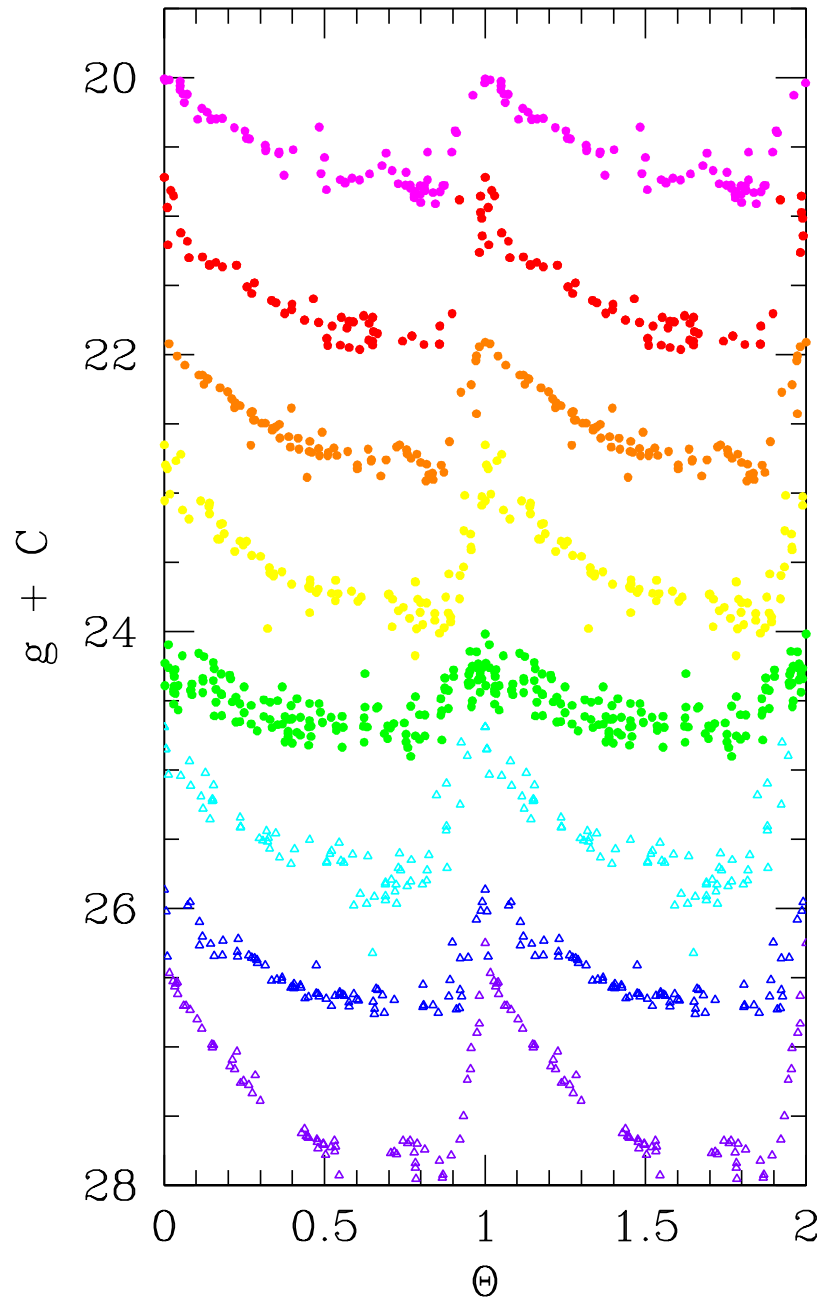


FIG. 2.— Lightcurves for targeted RR Lyrae stars in Stripe-82. Lightcurves are ordered as they appear in Table 1. The top five are part of the common-velocity structure near -75 km s^{-1} .

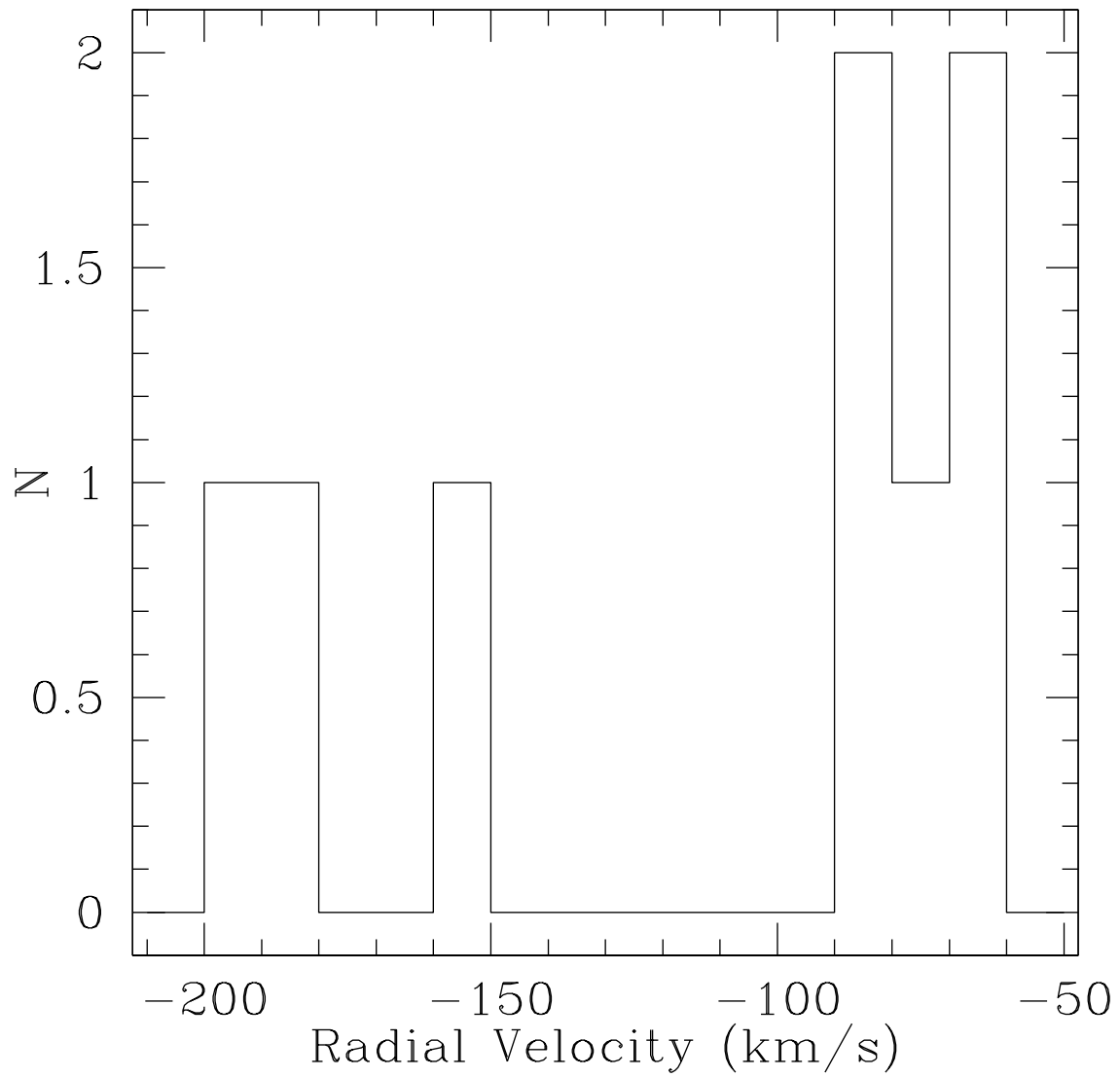


FIG. 3.— Histogram of heliocentric radial velocities for 8 RR Lyrae stars in the Pisces Overdensity. The concentration at -75 km s^{-1} is obvious. The clump at $\sim -190 \text{ km s}^{-1}$ is also of note.

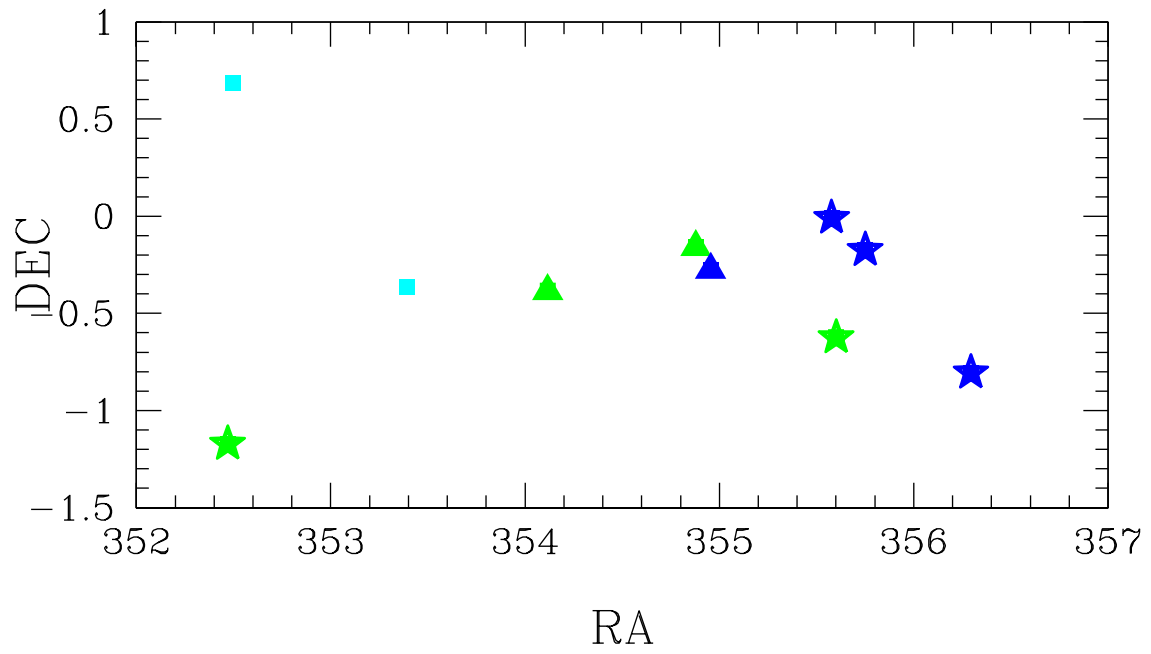


FIG. 4.— RR Lyrae targets for this program. Green, blue, cyan symbols correspond to median magnitude ranges of $20.5 \leq g_{med} < 20.6$, $20.6 \leq g_{med} < 20.7$, $g_{med} > 20.7$. Star symbols correspond to targets with velocity greater than -90 km s^{-1} and triangles are all other targets for which we have obtained a radial velocity. Squares show objects for which we do not yet have spectra.